

## Rapid detection by FTIR spectroscopy of the competition of Hg (II) and Pb (II) on the functional sites of humic acid.

M.C. Terkhi, M.R. Ghezzer, A. Addou\*

Laboratory of Science and Technical Environment and Valorization, University Abdelhamid Ibn Badis of Mostaganem, 27000, Algeria.

\* Corresponding author: ahmed.addou@univ-mosta.dz; Tel.: +213 0663141551

### ARTICLE INFO

#### Article History :

Received : 09/05/2020  
Accepted : 02/02/2021

#### Key Words:

Humic acid;  
Binary Hg- Pb competition;  
Affinity;  
FTIR Spectroscopy.

### ABSTRACT/RESUME

**Abstract:** This work shows that infrared spectroscopy is an easy and fast analytical technique for monitoring the behavior of the humic acids Fluka (impure) and Leonardite (pure) in contact with binary solutions of mercury and lead. The results showed the high fixation capacity of humic acids for mercury compared to lead and the adsorption rate of Fluka is always higher (for Hg 99%; and lead 96%) than Leonardite (Hg 70%; lead 42%). The spectra showed a shift ( $30\text{ cm}^{-1}$ ) of the asymmetric stretching vibration band from the carboxylate function  $-\text{COO}^-$  for the humic acids Fluka-binary solution interaction. In the case of mercury alone, the shift was of  $40\text{ cm}^{-1}$  and has decreased by  $10\text{ cm}^{-1}$ . That is proves that the cationic exchange becomes more difficult. The spectra also showed the variation of the intensity of the  $\text{C}=\text{O}$  elongation vibration band of the carboxylic function  $-\text{COOH}$  up to  $1610\text{ cm}^{-1}$  for the Leonardite humic acid-binary interaction. The high concentration of the binary solution did not result in the total disappearance of the  $\text{C}=\text{O}$  band as in the Leonardite humic acid-mercury alone interaction study. This proves that some carboxylic sites are not accessible to  $\text{Hg}^{2+}$  ions. These results were confirmed by monitoring the pH before and after ion exchange during the humic-binary acid (Hg-Pb) interaction. It appears that the  $-\text{COONa}$  or  $-\text{COOCa}$  to  $-\text{COOM}$  type transitions in Fluka humic acid were easy rather than the  $-\text{COOH}$  to  $-\text{COOM}$  type transitions in Leonardite humic acid.

### I. Introduction

Soil pollution by heavy metals including mercury and local may be due to negligence, ignorance of the danger level of pollutants or accident during industrial activities causing ecological damage and pollutes holdings of sites and areas surrounding [1]. Human action has resulted in increased concentrations of heavy metals in the environment. These high concentrations are of concern because they pose risks to human health, as well as to animals and plants [2]. Heavy metals: Cd, Hg, As,

Cu and Pb being the five most damaging metallic pollutants [3]. The soil consists of solid elements of mineral and organic nature including humic acid (HA).

Humic acids are complex and heterogeneous mixtures that can give rise to adsorption, ion exchange or even complex through surface oxidation-reduction reactions [4]. They are involved in the transport of a large number of chemical elements in the form of complexes or colloids. The HA is responsible for binding and metal release and manage mobility and bioavailability of metals [5,6].

In nature, several heavy metals may be available at the same time in soils. Therefore, the evaluation of adsorption simultaneous of these cations by the

organic matter is very important. For two decade, it was found that many studies (Table 1) focused on the follow-up of the metal competition to be adsorbed on the organic matter of the soil. Nevertheless, the participation of mercury in the competition with lead alone and Fluka humic acid (FHA) or Leonardite humic acid (LHA) is relatively absent from table 1, it is seen that Pb is the most favorable divalent meta to bind to the macromolecule organics.

There is significant sorption between Hg and Pb and HA [13,14].

The objective of our work is to study by FTIR the competition of fixation of Hg and Pb on HA on the one hand, and to follow the behavior of the latter in a binary Hg-Pb mixture. Through this study, we can easily and quickly detect by infrared whether a soil or solid sample containing humic acid is polluted with lead, mercury or both.

The FTIR spectroscopy technique is a fast and simple technique. It can provide a considerable insight into the structural arrangement of oxygen and carbon in humic acids [14,15]. Given the

complexity of the structure of humic acids, it was forced to do a study on model molecules. The latter are not representative of the functional groups of humic acid because of its highly complex structure, but they represent distinct classes of the exchange sites, with a binding affinity that can be similar. The molecules we selected for this study of HA-binary interaction (Hg, Pb) are benzoic acid, catechol and salicylic acid [13]. To approach the complex structure of humic acid we have added two other model molecules containing three aromatic rings: Xanthene 9-carboxylic acid and Anthralin. The HA-Metals interaction was followed firstly by the non-imposed pH before and after the HA-binary mixture (Hg, Pb) and secondly by FTIR.

The studies are focusing on competition focus on metals that have a difference in affinity for humic acid. No study has been carried out on the competition between humic acid and the bivalent heavy metals Hg and Pb which have a high affinity with humic acid as it is mentioned in Table 1. The results of the infrared study were confirmed by the ICP-AES analyzes of the metal cation exchanged.

**Table 1.** Adsorption competition between different bivalent cations

Adsorbent materials	Ranking in descending order	References
Purified Humic Acid	Pb>Cu>Cd	[7]
Humic Umbrisol	Pb>Cr>Cu>Cd≈Ni≈Zn	[8]
Humic Acids	Pb>Cu>Cd>Zn	[9]
Untreated Low-Rank Coal	Pb>Cu>Cd>Zn>Ni>Co	[10]
Humic Substances (compost)	Pb>Cu≈Zn>Ni>Cd	[11]
Humic Acid (compost)	Pb>Cd>Zn>Cu	[12]

## II. Materials and Methods

### II.1. Interaction model molecules - binary (Hg, Pb)

The model molecules that we adopted were chosen on the basis of the results of Shulten and Shnitzer [16] which showed that HA is a complex macromolecule containing several aromatic rings which carry carboxylic and salicylic functions while the phenolic functions are grafted on the aliphatic

chains. N and S elements, although they also play a significant role in the interaction with heavy metals [17], were not included in our models. Our choice fell on two series: The 1st is composed of a single aromatic ring (benzoic acid, catechol and salicylic from (Merck)). The 2nd is composed of three aromatic rings (Xanthene 9-carboxylic acid and Anthralin: from Aldrich). The developed formulas of the model molecules are shown in Figure 1.

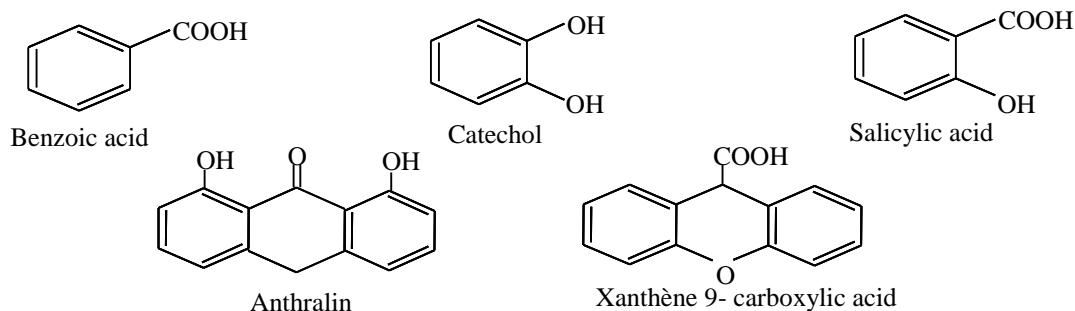


**Figure 1.** Schematic representation of the developed formula of the model molecules.

For all these model molecules, the preparation of the mercury and lead salts was done in the same way according to the following procedure: 1g of each model compound in its acid form is neutralized with NaOH 2M to which is added either a solution of mercury nitrate 1M (from Fluka) or lead nitrate 1M (Fluka) or a mixture of both solutions (Binary). The addition of each solution allowed the precipitation (white solid) of the carboxylate and phenolate of mercury and lead. These salts were then studied by FTIR spectroscopy and compared to their acid form. 2g of each precipitate was dried at 80°C and milled in 100 mg of anhydrous KBr. The powder obtained was placed in a mold to be pelletized and subjected to a pressure of  $9.81 \times 10^8$  Pa. The pellet of 13 mm diameter was analyzed directly by FTIR spectroscopy. The spectrometer used is a Bruker YEWS 48. We worked in the range 400-4000  $\text{cm}^{-1}$  with a resolution of 4  $\text{cm}^{-1}$ .

## II.2. Characterization of humic acids

The commercial humic acid studied is supplied by Fluka (FHA) (45729/150300). The second humic acid used is the Leonardite (LHA) provided by the International Humic Substances Society (IHSS, Nord Dakota, USA). It was isolated by IHSS protocol [18]. Chemical and spectroscopic FTIR analyzes were used to characterize the studied humic acids:

- (i) Basic tests to detect C, H, N, S and O present in the AHF by CHNS elemental analyzer LECO type (Laboratory Equipment Corporation) Model 932. This apparatus uses samples of the order of 2 to 5 mg. The elementary compositions of LHA were performed by Huffman Laboratories, Inc., Wheatridge, CO.
- (ii) The analysis of the acidity of the carboxylic functions was carried out by the calcium acetate technique as well as the determination of the total acidity by barium hydroxide [19]. Each analysis was repeated three times;
- (iii) The analysis of metals (Na, Ca, Fe, Mg, Si and Al) commonly found in FHA and LHA in addition to mercury and lead was carried out by ICP-AES (Varian, axial view, liberty series V);
- (iv) The calculation of ash was determined in our previous works [13, 14]; (v) Humic acids FHA and

LHA were analyzed by FTIR spectrometry before interaction with the solution of mercury or lead. We have used the same pelletizing technique with KBr in the study of model molecules.

## II.3. Interaction Humic acid–binary (Hg, Pb)

200 mg of Humic Acid (FHA or LHA) were added to 50 ml of solution of Milli-Q water. The procedure of humic acid interaction with mercury and lead mixed solution in the same. Mercury solution were obtained from mercury nitrate solutions with concentrations of 0.1, 0.5 and 1.0 g/l. Lead solutions were prepared from lead nitrate at the concentrations of 0.1, 0.5 and 1.0 g/l. Three binary systems (Hg, Pb) at three different concentrations were prepared in ratios of 1:1 (0.1; 0.5 and 1 g/l). 200 mg of HA (FHA or LHA) were added to 50 ml of the mixed solution Hg-Pb. Eight samples were thus obtained including the control. The initial pH was measured immediately after addition of the solution of simple or mixed metal about 200 mg of HA. The final pH was measured after 24 hours of stirring time. This is followed by centrifugation of 2400  $\text{tr.min}^{-1}$  for 1 hour. The solid parts (HA + metals fixed) are dried at 80°C during 16 h. After drying, the solid parts can be analyzed by FTIR spectroscopy. The recovered supernatants are determined by ICP-AES to determine the remaining amounts of mercury and lead metal and other mineral elements Na, Ca, Fe, Mg, Si and Al. All experiments were repeated three times in the same temperature of 25°C.

## III. Results and discussion

### III.1. FTIR analyses of the interaction model molecules-metal single and binary

FTIR spectroscopy (Figures 2 and 3) shows clearly the acidic forms (bands related to carboxylic acids and phenols) of model molecules in their pure state. Several works confirmed the positions of the bands of its forms [20-22].

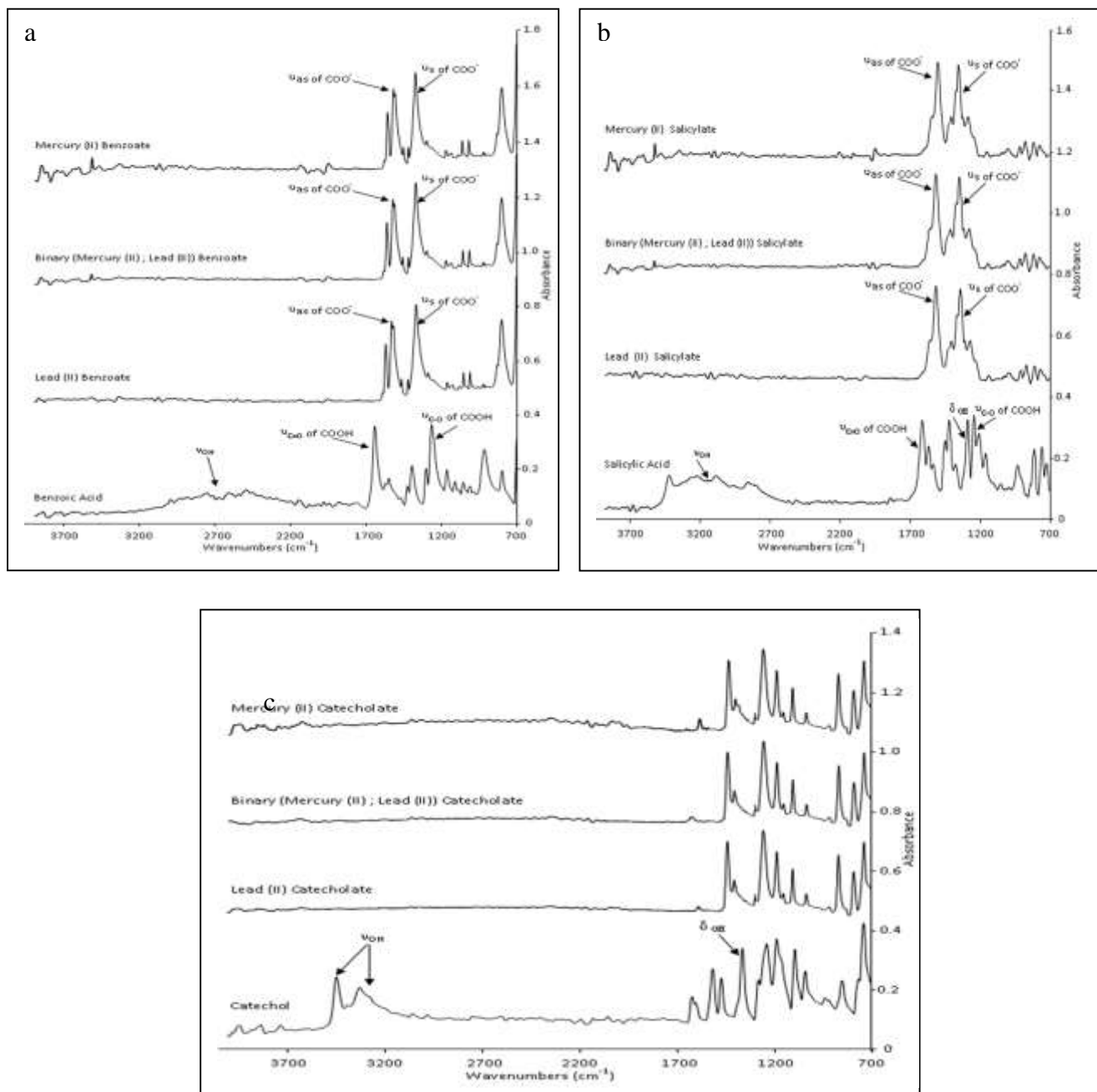


**Figure 2.** FTIR spectra of model molecules with an aromatic ring before and after interaction with mercury and lead: (a) Benzoic, (b) acid salicylic acid and (c) Catechol.

The FTIR spectra show the strong polarity of the C=O bond of the -COOH function which makes it very intense and therefore very recognizable. The vibration of elongations  $\nu_{C=O}$  corresponding appears between about 1700 and 1650 cm<sup>-1</sup>. While the

$\nu_{C=O}$  elongation vibrations of the acid function are observed between 1300-1230cm<sup>-1</sup>. The hydroxyl forms are assigned to large bands in 3400-3200 cm<sup>-1</sup> range, due to O-H stretching. The other characteristic bands are O-H deformation vibrations of phenol or alcohol type in about 1380-1330 cm<sup>-1</sup> range.

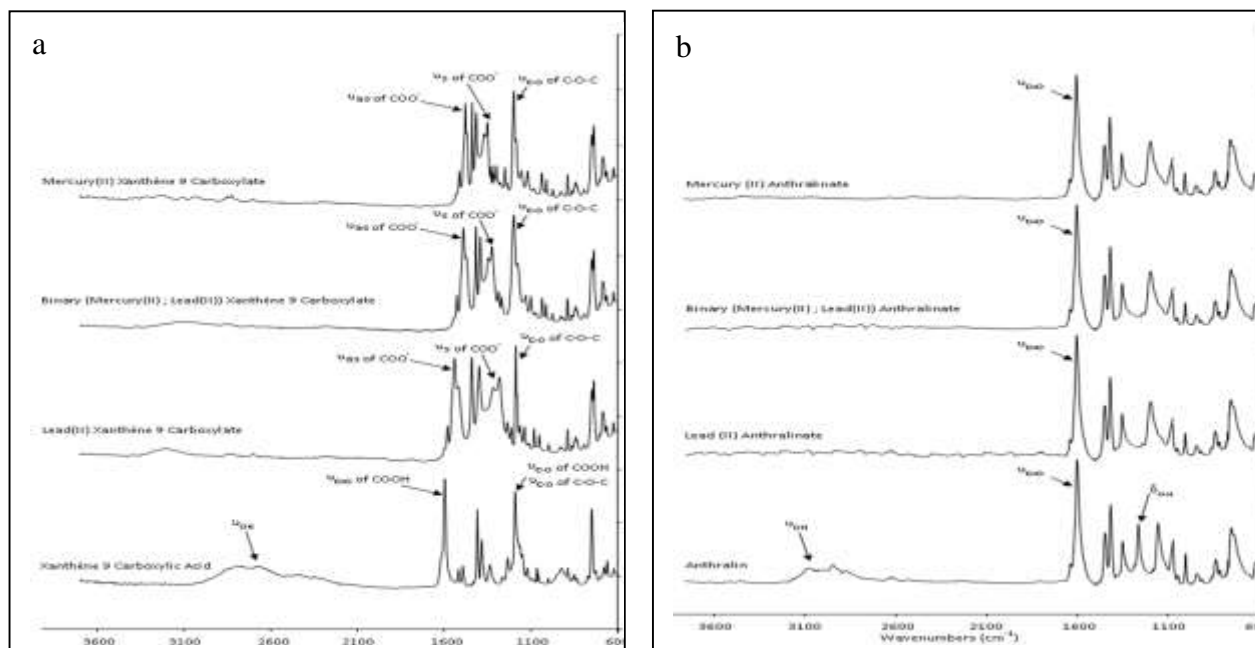


**Figure 3.** FTIR spectra of model molecules with three aromatic rings before and after interaction with mercury and lead: (a) Xanthine 9 Carboxylic Acid and (b) Anthralin.

The interaction of the model molecules with the heavy metals Hg, Pb or binary Hg-Pb caused the shift of the characteristic peaks of the carboxylate function according to the corresponding metal ion.

Indeed, the frequency of the  $\nu_{as}$  changes from 1593 to 1496  $\text{cm}^{-1}$  and that of the  $\nu_s$  varies from 1390 to 1361  $\text{cm}^{-1}$  (Table 2). This shift was confirmed by the calculation of frequency separations  $\Delta\nu_{as-s}$  between the  $\nu_{as}$  and  $\nu_s$  [23].

**Table 2.** Assigning bands of the main functions of model molecules before and after interaction with Hg [13], Pb [14] and binary (Hg-Pb)

Function	-COOH		-OH		-COO <sup>-</sup>			C=O	C-O-C	
	$\nu_{C=O}$	$\nu_{C-O}$	$\nu_{O-H}$	$\delta_{O-H}$	$\nu_{as}$	$\nu_s$	$\Delta\nu_{as}$	$\nu_{C=O}$	$\nu_{as}$	$\nu_s$
Vibration of the function	cm <sup>-1</sup>	cm <sup>-1</sup>	cm <sup>-1</sup>	cm <sup>-1</sup>	cm <sup>-1</sup>	cm <sup>-1</sup>				
Unit	cm <sup>-1</sup>	cm <sup>-1</sup>	cm <sup>-1</sup>	cm <sup>-1</sup>	cm <sup>-1</sup>	cm <sup>-1</sup>				
Benzoicacid	1676	1230	2500-3200	-	-	-	-	-	-	-
Benzoicacid + Hg <sup>+2</sup>	-	-	(-) <sup>a</sup>	-	1496	1390	106	-	-	-
Benzoic acid + Binary (Hg <sup>+2</sup> ,Pb <sup>+2</sup> )	-	-	(-) <sup>a</sup>	-	1498	1380	118	-	-	-
Benzoicacid + Pb <sup>+2</sup>	-	-	(-) <sup>a</sup>	-	1500	1365	135	-	-	-
Catechol	-	-	3442-3318	1359	-	-	-	-	-	-
Catechol + Hg <sup>+2</sup>	-	-	(-) <sup>a</sup>	(-) <sup>a</sup>	-	-	-	-	-	-
Catechol + Binary (Hg <sup>+2</sup> ,Pb <sup>+2</sup> )	-	-	(-) <sup>a</sup>	(-) <sup>a</sup>	-	-	-	-	-	-
Catechol + Pb <sup>+2</sup>	-	-	(-) <sup>a</sup>	(-) <sup>a</sup>	-	-	-	-	-	-
Salicylicacid	1658	1249	3200-3400	1380	-	-	-	-	-	-
Salicylicacid + Hg <sup>+2</sup>	-	-	(-) <sup>a</sup>	(-) <sup>a</sup>	1554	1384	170	-	-	-
Salicylic acid + Binary (Hg <sup>+2</sup> ,Pb <sup>+2</sup> )	-	-	(-) <sup>a</sup>	(-) <sup>a</sup>	1565	1375	190	-	-	-
Salicylicacid + Pb <sup>+2</sup>	-	-	(-) <sup>a</sup>	(-) <sup>a</sup>	1593	1361	232	-	-	-
Xanthène 9 CarboxylicAcid	1670	1233	2900-3300	-	-	-	-	-	1233	1030
Xanthène 9 CarboxylicAcid + Hg <sup>+2</sup>	-	-	(-) <sup>a</sup>	-	1500	1383	117	-	1236	1030
Xanthène 9 Carboxylic Acid + Binary (Hg <sup>+2</sup> ,Pb <sup>+2</sup> )	-	-	(-) <sup>a</sup>	-	1513	1374	139	-	1233	1030
Xanthène 9 CarboxylicAcid+ Pb <sup>+2</sup>	-	-	(-) <sup>a</sup>	-	1585	1308	277	-	1235	1030
Anthralin	-	-	2950-3100	1330	-	-	-	1604	-	-
Anthralin + Hg <sup>+2</sup>	-	-	(-) <sup>a</sup>	(-) <sup>a</sup>	-	-	-	1601	-	-
Anthralin + Binary (Hg <sup>+2</sup> , Pb <sup>+2</sup> )	-	-	(-) <sup>a</sup>	(-) <sup>a</sup>	-	-	-	1601	-	-
Anthralin + Pb <sup>+2</sup>	-	-	(-) <sup>a</sup>	(-) <sup>a</sup>	-	-	-	1603	-	-

<sup>a</sup>Disappearan

### III.1.1. Molecules models composed of a single aromatic ring

#### III.1.1.1. Benzoic acid and salts

The FTIR spectra of benzoic acid and their metal salts presented in Figure 2a shows the main characteristic attributions of the carboxylic function and carboxylate. The attributions are summarized in Table 2. The vibration elongations C=O and C-O of the COOH function were observed respectively at 1676 and 1230 cm<sup>-1</sup>. There is also a large band  $\nu_{OH}$  of acids between 3200-2500 cm<sup>-1</sup>. For the benzoic spectra of the salified acid (Hg, Hg-Pb, Pb), we have observed two major changes in

comparison with the spectrum of benzoic acid disappearance of the bands  $\nu_{OH}$ ,  $\nu_{C=O}$  and  $\nu_{CO}$  of carboxylic function in favor of the two elongation vibration bands characteristics of the carboxylate functions -COOM which are :

- (i) The  $\nu_{C-O}$  symmetrical ( $\nu_s$ ) at 1390 cm<sup>-1</sup> for the mercury salt at 1380 cm<sup>-1</sup> for the binary salt and 1365 cm<sup>-1</sup> for the lead salt,
- (ii) The  $\nu_{C-O}$  asymmetric ( $\nu_{as}$ ) at 1496 cm<sup>-1</sup> for the mercury salt and at 1498 cm<sup>-1</sup> for the binary salt and at 1500 cm<sup>-1</sup> for the lead salt.

After interaction of benzoic acid with metal solutions, symmetric C-O peak shift to large wave numbers and asymmetric  $\nu_{C-O}$  peak shift towards low wave numbers were observed. This shift in the case of mercury alone was higher than for lead alone. Thus values of  $\Delta\nu_{as-s}$  for the salts of Hg and Hg-Pb binary and Pb are of 16, 118 and 135  $cm^{-1}$ , respectively (Table 2). The benzoic acid thus has an affinity with mercury relative to lead. This affinity was disrupted by the presence of mercury and lead as the shift was reduced.

### III.1.1.2. Salicylic acid and salts

FTIR spectra of salicylic acid and its salts of mercury, binary (mercury-lead) and lead (Figure 2b) show that the two elongation frequencies of the function  $-COOH$  ( $\nu_{C-O}$ ) at 1658  $cm^{-1}$  and  $\nu_{C-O}$  at 1249  $cm^{-1}$  have been replaced by those of  $\nu_{as}$  of the function  $-COO^-$  at 1554  $cm^{-1}$  for the mercury salt, at 1565  $cm^{-1}$  for the binary and at 1593  $cm^{-1}$  for the lead salt. Vibration  $\nu_s$  of the same function  $-COO^-$  appears at 1384  $cm^{-1}$  for the mercuric salicylate at 1375  $cm^{-1}$  for binary salicylate and at 1361  $cm^{-1}$  for lead salicylate (Table 2). There is an important shift of  $\nu_s$  and  $\nu_{as}$  for the case of the salicylic acid-mercury interaction alone indicating the power of mercury in front of lead alone. This affinity was slowed in the presence of mercury and lead since the shift of the elongation peak  $\nu_{as}$  and  $\nu_s$  has decreased with 10  $cm^{-1}$ . This diminution is caused by the increase of the  $\Delta\nu_{as-s}$  (170  $cm^{-1}$ ) for the Hg salt at 190  $cm^{-1}$  in the binary Hg-Pb salt. If we compare the FTIR spectra of salicylic acid and its metal salts studied, we can see the complete disappearance of the  $\nu_{OH}$  stretching frequencies observed between 3400-3200  $cm^{-1}$  and the deformation  $\delta_{OH}$  at 1380  $cm^{-1}$ .

### III.1.1.3. Catechol and salts

The FTIR spectrum catechol shown in Figure 2c indicates the presence of the hydroxyl function characterized by two major bands. The first is the  $\delta_{OH}$  bending vibration at 1359  $cm^{-1}$ , the second has  $\nu_{OH}$  stretching frequency at 3442  $cm^{-1}$  and 3318  $cm^{-1}$ . The catechol-metal interaction (single or binary) has removed the two characteristic bands of the phenol form.

## III.1.2. Model molecules with three aromatic rings

### III.1.2.1. Xanthene 9 Carboxylic Acid and salts

The FTIR spectrum of xanthene 9 carboxylic acid (Figure 3a) showed the corresponding adsorption band to the  $-COOH$  function which appears at 1670  $cm^{-1}$  for the elongation vibration  $\nu_{C=O}$ . While the

stretching vibration  $\nu_{C-O}$  of the same acid function is observed strongly at 1233  $cm^{-1}$  (Table 2) which may also be characteristic of the  $\nu_{C-O}$  asymmetric ( $\nu_{as}$ ) of the ether function C-O-C. On the other hand the  $\nu_{C-O}$  symmetric ( $\nu_s$ ) of the ether function C-O-C is observed weakly at 1030  $cm^{-1}$ . The FTIR spectrum of xanthene 9 carboxylic acid also shows an absorption band corresponding to the OH function that appears between 2900 and 3300  $cm^{-1}$  presented in the form of a wide band.

After the fixation of Hg, Pb and the binary Hg-Pb, we have noticed: (i) the disappearance of the bands of the carboxylic and hydroxyl functional groups and (ii) the shifts of the asymmetric elongation the low frequencies corresponding to the salts of mercury, binary Hg-Pb and lead. They are observed respectively at 1500, 1513 and 1585  $cm^{-1}$  (Table 2). For the symmetrical elongation  $\nu_s$  of  $-COO^-$  they are attributed to 1383, 1374 and 1308  $cm^{-1}$  bands. These shifts show that mercury was able to easily form complexes compared to lead. Indeed, the peak characteristic of  $\nu_{as}$  of  $-COO^-$  was displaced by 170  $cm^{-1}$  for mercury alone. For the binary solution, the shift was of 157  $cm^{-1}$  and only 85  $cm^{-1}$  for lead alone. The shifts observed in the pics of  $\nu_{as}$  and  $\nu_s$  have caused the increase of  $\Delta\nu_{as-s}$  of 117 until 227  $cm^{-1}$  for the Hg and Pb salts, respectively. This is probably due to the interaction between  $COO^-$  and  $Hg^{2+}$  which is more important than that between  $COO^-$  and  $Pb^{2+}$ . It can be seen in Figure 3a that the characteristic bands of the ether function are always present before and after Xanthene 9 carboxylic acid-metal interaction.

### III.1.2.2. Anthralin and salts

The FTIR spectra of anthralin and its salt forms are grouped together in Figure 3b and the main frequencies corresponding are summarized in Table 2. We have noted the deformation frequencies  $\delta_{OH}$  of the OH function at 1330  $cm^{-1}$ , the elongation frequency  $\nu_{OH}$  of the OH function between 2950-3100  $cm^{-1}$  and an intense frequency at 1604  $cm^{-1}$  which corresponds to the elongation vibrations  $\nu_{C=O}$  of the function  $-C=O$  [24]. The interaction with the mercury, lead, and the binary Hg-Pb results to the formation of anthralinate which the elongation characteristic band  $\nu_{O-H}$  and the deformation  $\delta_{OH}$  disappear completely. On the other hand, the characteristic peak of the  $C=O$  function has not varied.

### III.2. Summary analyses by FTIR

These model molecules do not make possible the characterization of a real behavior between the macromolecule of humic acid type and heavy metals. The study of these models has validated, on the one hand, the use of FTIR for a certain type of interaction and, on the other hand, to help the characterization with a systematic interpretation of FTIR spectra of more complex molecules. Indeed, the FTIR spectra (Figures 2 and 3) show two main behaviors during the study of the interaction of model metal molecules (single or binary): (i) The easy monitoring of the frequency band related to COO to the vibration of asymmetric and symmetric elongation carboxylates in the region 1700 and 1383  $\text{cm}^{-1}$ . This frequency depends on the fixed metal cation [39]. We have noted for model molecules with carboxylic functions, that the wave numbers of asymmetric vibrations  $\nu_{\text{as}}$  ( $-\text{COO}^-$ ) of Hg are lower than those of the binary (Hg, Pb) and Pb alone. The  $\nu_{\text{s}}$  frequency of the Hg salt is higher than the Hg-Pb binary and Pb salts frequencies.

This suggests that mercury alone is easily attached to the COOH functional sites of the model under study. These frequencies are disturbed by the presence of lead which is probably due to the competition between these two metals to occupy these functional carboxylic sites. Liu et al. [25] found similar results when studying the interaction of peat with mixed solutions of Cu, Ni and Cd.

They attributed this competition to the repulsive electrostatic forces.

(ii) In the case of the interaction of the model molecule which contains only an OH function with the single or binary metal, the disappearance of the characteristic bands of the hydroxyl function was observed. Inhibition of mercury binding in the presence of lead was not clearly visible in the FTIR spectra (Figures. 2 and 3). In a previous work, Bosire et al. [26] confirmed the important role of acidic functions in forming bonds with Pb, Cu and Zn. Phenol sites were the least involved because their acidity constants were low.

Our study by FTIR spectroscopy has the advantage of easily following the evolution of the characteristic bands of asymmetric elongations  $\nu_{\text{as}}$ , of symmetric elongations  $\nu_{\text{s}}$  and of the carboxylate function and  $\nu_{\text{C}=\text{O}}$  of the carboxylic function to study the interactions between FHA, LHA and heavy metals.

### III.3. Comparison of the characteristics of the studied humic acids

#### III.3.1. Elementary, ash content results, functional group and ICP-AES determination

Elementary analysis of C, H, N, S and O (Table 3) showed results closer values announced by Steelink [27]. The oxygen level is still relatively high for FHA, it is well above the range of 32.8-38.3% usually found.

**Table 3.** Elemental, ash content results and acidity analysis of used humic acids

Elements	FHA	LHA	Steelink [27]
C <sup>a</sup>	44.94	63.25	53.8-58.7
H <sup>a</sup>	3.84	3.64	3.2-6.2
N <sup>a</sup>	0.75	1.17	0.8-4.3
S <sup>a</sup>	1.10	0.84	0.1-1.5
O <sup>a</sup>	49.35	31.05	32.8-38.3
C/N	59.92	54.06	-
H/C	0.08	0.06	-
O/C	1.10	0.50	-
Ash content <sup>b,c</sup>	19.7	2.58	-
Total acidity <sup>d</sup>	4.62	7.10	-
R-COOH <sup>d</sup>	4.20	6.84	-
R-OH <sup>d</sup>	0.42	0.26	-

<sup>a</sup> % Mass of the element by the total mass.

<sup>b</sup> % Mass of the element by the total mass.

<sup>c</sup> Calculated by the combustion of 100 mg HA in air at 800 °C for 6h.

<sup>d</sup> Units are mol/kg HA.

Table 4 also shows that FHA contains almost 100 times the amount of Si as LHA and 2 times more aluminum than LHA. This shows the presence of the mineral part as an impurity such as:  $\text{SiO}_2$ ,  $\text{Al}_2\text{O}_3$  and  $\text{Fe}_2\text{O}_3$ . The ash content of 19.7% in FHA confirms the presence of these oxides. The amounts of oxygen in LHA are lower than those of FHA.

This is because LHA is pure, contains significantly less iron, aluminum or silicon oxides.

Similarly, the carbon content in FHA is well below the range of 53.8-58.7% and the nitrogen percentage is 0.75%. Thus, LHA contains more carbon (63.25%) and more nitrogen (1.17%) than FHA. Following the results of the elementary analysis, the

variation of the C/N ratios is obtained in the following order: LHA <FHA (54.06 <59.92). These values reflect a significant incorporation of nitrogen compounds in LHA. The O/C ratios vary according to the following sequence: FHA >LHA (1.10 >0.50). These values reflect the level of oxygenated functional groups of each of these compounds, which is explained by the fact that LHA contains The results of the total acidity and the content of carboxylic groups for humic acids (FHA, LHA) are grouped together in Table 4. The results of the carboxylic and phenolic functional determinations for FHA are respectively of the order of 4.20 and 0.42 mol/kg. The total acidity has been estimated at 4.62 mol/kg. The data in Table 4 also indicate that LHA is more acidic than FHA. The total acidity

significantly fewer iron, aluminum or silicon oxides. In parallel, the ICP-AES quantitative analysis of the two humic acids (Table 4) proves the purity of LHA and the sodium salt and calcium form of FHA. in fact, it contains a FHA does a significant amount of Na and Ca, of the order of 36800 and 21800 mg/Kg respectively while LHA has only 2000 mg/Kg of Na and 3000 mg/Kg of Ca. content in LHA was almost twice that of FHA. A possible explanation for the different elemental composition for the two humic acids can be found in their precursor materials and the influence of climatic conditions during the humification process [27].

**Table 4.** Cations titration of: the studied HA, sorption HA-mercury [13], sorption HA-lead [14] and sorption HA-Binary (mercury- lead).

FHA	0 g/l	Hg (1.0 g/l)	Pb (1.0 g/l)	(Hg-Pb) (1.0 g/l)
Na (mg/Kg)	36800	2000	2900	2500
Ca (mg/Kg)	21800	7600	8500	8050
Fe (mg/Kg)	13800	11000	12500	11750
Mg (mg/Kg)	4400	1500	2100	1800
Hg (mg/Kg)	0	248750	0	112500
Pb (mg/Kg)	60	60	240000	103750
Si (mg/Kg)	18000	15000	16000	15600
Al (mg/Kg)	9000	6500	7200	6900

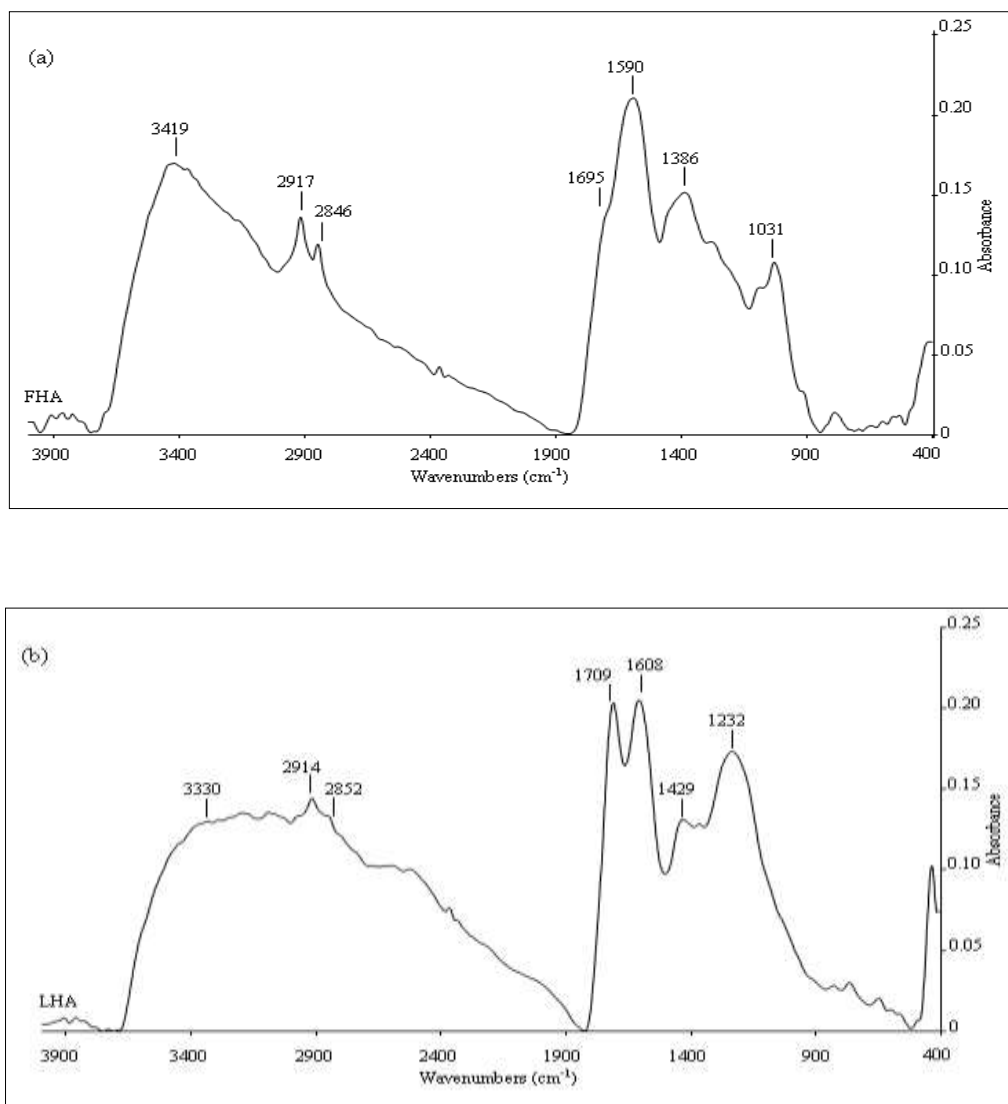
  

LHA	0 g/l	Hg (1.0 g/l)	Pb (1.0 g/l)	(Hg-Pb) (1.0 g/l)
Na (mg/Kg)	2000	170	200	185
Ca (mg/Kg)	3000	0	0	0
Fe (mg/Kg)	2000	995	1075	1035
Mg (mg/Kg)	40	0	0	0
Hg (mg/Kg)	0	175000	0	78750
Pb (mg/Kg)	65	65	104500	43750
Si (mg/Kg)	150	<150	<150	<150
Al (mg/Kg)	2500	<2500	<2500	<2500

### III.3.2. Vibrational characteristics

The analysis of the infrared spectra of the FHA and LHA humic acids are shown in Figure 4. The two spectra obtained have great similarities with respect to the general appearance and the positions of the main peaks. FTIR spectra can be divided into two main regions [28]. The first region (4000-1900 cm<sup>-1</sup>) is similar for FHA and LHA. It contains broad peaks characteristic of humic substances. They are attributed mainly to the elongation vibration  $\nu_{O-H}$

and  $\nu_{N-H}$ . Between 3450 and 3300 cm<sup>-1</sup>, phenol -OH elongation bands of hydrogen bonds can be observed. Between 2965 and 2840 cm<sup>-1</sup>, the spectra of the two acids show very weak vibration bands characteristic of the C-H aliphatic bond constituting -CH<sub>2</sub> and -CH<sub>3</sub>. In the second region (1900-400 cm<sup>-1</sup>), the FHA and LHA FTIR spectra change significantly and confirm the salt (impure) form of FHA and the (pure) acid form of LHA already found by elementary ICP-AES and functional group dosage.



**Figure 4.** FTIR spectra of: (a) Humic acid Fluka (FHA) and (b) Humic acid Leonardite (LHA).

Table 5 summarizes the main results in the characterization of the humic acids studied. The presence of the band corresponding to the extension of the C=O bond of the strong carboxylic acids to 1709 cm<sup>-1</sup> of LHA indicates its purity. However, it is absent in the spectrum of FHA thus confirming its salt form. The characteristic asymmetric elongation band  $\nu_{as}-\text{COO}^-$  appears at 1590 cm<sup>-1</sup>. The characteristic symmetric elongation band  $\nu_s-\text{COO}^-$  appears at 1386 cm<sup>-1</sup>.

The spectrum of FHA (Figure 4a) shows the Si-O elongation vibration band of silica located around 1031 cm<sup>-1</sup> indicating the presence of the mineral

part [20] (Table 5). This band is no longer visible in the case of LHA (Figure 4b) proving that it consists mainly of organic matter. This spectral information will be useful for the study of the behavior of organic matter (LHA) when interacting with metallic elements and observing their spectral changes. It should be noted that the mineral part of soils also has a high adsorption capacity of metals. Indeed, Babel et al. have shown the existence of a low-cost inorganic or organic adsorbents used for the removal of heavy metals [29].

**Table 5.** Summary of the main results of the different methods of analysis used in the characterization of the

Sample	Chemical analysis						Acidity	FTIR Spectroscopy				Information obtained	
	C (%)	O (%)	Na (mg/Kg)	Ca (mg/Kg)	Si (mg/Kg)	Ash (%)	R-COOH (mol/Kg)	$\nu_{C=O}$ COOH	$\nu_{as}$ COO <sup>-</sup>	$\nu_s$ COO <sup>-</sup>	$\nu_{Si-O}$ of silice	Forme of sample	Etat of sample
FHA	44.94	49.35	36800	21800	18000	19.7	4.20	Absence	1590 cm <sup>-1</sup>	1386 cm <sup>-1</sup>	1031 cm <sup>-1</sup>	Sel	Impure
LHA	63.25	31.05	2000	3000	150	2.58	6.84	1709 cm <sup>-1</sup>	1608 cm <sup>-1</sup>	1429 cm <sup>-1</sup>	Absence	Acide	Pure

studied humic acids

### III.4. Study of interactions HA-binary (Hg-Pb)

Tables 4 and 6 showed the results of analysis as a function of pH, adsorption percentages, the

characteristics of the function -COOH and -COO<sup>-</sup> and cation analysis before and after complexation.

**Table 6.** Chemical characterization of the sorption HA-mercury [13], HA-lead [14] and HA-Binary (mercury-Lead)

Humic Acid	Initial Concentration of métal	Adsorption system	Initial pH	Final pH	Mass adsorbed (mg)	% of adsorption	
FHA	0 g/l	Blank	4.45	6.50	0.0	0.0	
	0.1 g/l	Hg	5.27	6.20	4.55	91	
		Pb	5.25	6.18	4.50	90	
		<b>Hg (Hg,Pb)</b>	<b>5.27</b>	<b>6.20</b>	<b>2.22</b>	<b>89</b>	
		<b>Pb (Hg,Pb)</b>	<b>5.27</b>	<b>6.20</b>	<b>2.12</b>	<b>85</b>	
	0.5 g/l	Hg	5.03	5.22	23.75	95	
		Pb	5.05	5.19	23	92	
		<b>Hg (Hg,Pb)</b>	<b>5.00</b>	<b>5.16</b>	<b>11.37</b>	<b>91</b>	
		<b>Pb (Hg,Pb)</b>	<b>5.00</b>	<b>5.16</b>	<b>11</b>	<b>88</b>	
	1.0 g/l	Hg	4.80	4.25	49.50	99	
		Pb	4.86	4.21	48	96	
		<b>Hg (Hg,Pb)</b>	<b>4.84</b>	<b>4.24</b>	<b>22.50</b>	<b>90</b>	
		<b>Pb (Hg,Pb)</b>	<b>4.84</b>	<b>4.24</b>	<b>20.75</b>	<b>83</b>	
	LHA	0 g/l	Blank	5.60	3.16	0.0	0.0
		0.1 g/l	Hg	5.00	2.92	4.85	97
Pb			5.02	2.95	4.1	96	
<b>Hg (Hg,Pb)</b>			<b>5.00</b>	<b>2.93</b>	<b>2.37</b>	<b>95</b>	
<b>Pb (Hg,Pb)</b>			<b>5.00</b>	<b>2.93</b>	<b>2.27</b>	<b>91</b>	
0.5 g/l		Hg	4.98	2.50	19	75	
		Pb	5.00	2.57	12.8	52	
		<b>Hg (Hg,Pb)</b>	<b>5.00</b>	<b>2.55</b>	<b>8.87</b>	<b>71</b>	
		<b>Pb (Hg,Pb)</b>	<b>5.00</b>	<b>2.55</b>	<b>6.25</b>	<b>50</b>	
1.0 g/l		Hg	4.96	2.20	35	70	
		Pb	4.99	2.40	21	42	
		<b>Hg (Hg,Pb)</b>	<b>4.98</b>	<b>2.29</b>	<b>15.75</b>	<b>63</b>	
		<b>Pb (Hg,Pb)</b>	<b>4.98</b>	<b>2.29</b>	<b>8.75</b>	<b>35</b>	

### III.4.1. Study of interactions FHA-binary (Hg-Pb)

#### III.4.1.1. Influence of the concentration of the mixed solution Hg-Pb

Data from the study of FHA-Metal interactions alone or binary at different concentrations 0.1, 0.5

and 1 g/l are grouped in Table 6. The results show that:

- (i) For a mixed solution to a concentration of 0.1 g/l mercury and 0.1 g/l of lead, the fixation percent of mercury and lead was respectively of the order of 89% and 85%.

(ii) When the concentration of mercury and lead increases in the mixture (0.5 g/l), the fixation percentage of these metals increase slightly by 3%.

(iii) A concentration of g/l of the mixed solution, the percentage of binding is 90% for mercury and 83% for lead.

For these three concentrations, it was noted that the fixed quantity in the case of binary Hg-Pb never reached the maximum quantities fixed, as for the case of mercury alone (99%) and lead alone (96%). The active sites FHA are not all available in the case of the binary solution. This is probably due to the competition and the repulsive electrostatic forces between the two ions  $\text{Hg}^{2+}$  and  $\text{Pb}^{2+}$ . This suggests that the maximum percentage of adsorption in the binary solution follows the following order:  $\text{Hg (Hg-Pb)} > \text{Pb (Hg-Pb)}$ .

The second between protons carboxylic functions and metals once the carboxylate functions were exhausted. The release of protons present in small quantities in FHA was the main cause of the decrease in pH. In this step we can say that FHA has undergone a larger fixation. We also noticed that the decrease was considerable in consideration of the FHA interaction with mercury or lead alone with respect to the mixed solution Hg-Pb. If we take for example the fixing of mercury alone (1 g/l) by FHA, we only have  $\text{Na}^+$  (2000 mg/Kg) and  $\text{Ca}^{2+}$  (7600 mg/Kg) (Table 4). The pH filled from 4.8 to 4.25 (Table 6). For the mixed solution Hg-Pb, the change of the form  $-\text{COO-Na}$  or  $-\text{COO-Ca}$  to the form  $-\text{COO-Hg}$  became difficult due to the presence of lead. This inhibition phenomenon is demonstrated by the remaining amount of  $\text{Na}^+$  (2500 mg/Kg) and  $\text{Ca}^{2+}$  (8050 mg/Kg). The data in Tables 4 and 6 also showed that the ion exchange between  $\text{Pb}^{2+}$  and the  $\text{Na}^+$  and  $\text{Ca}^{2+}$  cations was disrupted by the presence of mercury in the study of the FHA-binary interaction Hg-Pb. The  $\text{Na}^+$ ,  $\text{Ca}^{2+}$  dosage, final pH and adsorption percentage values were always lower than those of the FHA-Pb interaction.

#### III.4.1.3. FTIR Spectroscopy monitoring

Examination of the infrared spectra (Figure 5a) of the complex formed by Fluka humic acid and the Hg and Pb mixture showed the same pattern for the ten spectra found. It has been found that:

#### III.4.1.2. Initial and final pH

The previous sequence was confirmed by pH monitoring (Table 6). Indeed, at the same concentrations of 0.1 g/l and 0.5 g/l of mixed mercury and lead solution, the final pH is always higher than the initial pH. The increase in the final pH is due to the release of the  $\text{Na}^+$  and  $\text{Ca}^{2+}$  cations present in the AHF during the exchange with the metal  $\text{Hg}^{2+}$  and  $\text{Pb}^{2+}$  ions (Table 4). This increase was slowed in the case of the binary system Hg-Pb.

The study of FHA interactions with individual or mixed solutions at high concentration (1g/l) showed that the initial pH is always lower than the final pH. It has been concluded that is ion exchange goes through two stages: The first between the  $\text{Na}^+$  and  $\text{Ca}^{2+}$  cations, by FHA carboxylate functions and the two metals (Table 4).

(i) The intensity of elongation absorption band  $\nu_{\text{C=O}}$  at  $1695 \text{ cm}^{-1}$  of the carboxylic function did not vary after the interaction of FHA (salt form), regardless of the concentrations of the studied solutions (Table 6). (ii) The shift of the vibration band elongation symmetrical  $\nu_s$  initially located at  $1386 \text{ cm}^{-1}$  of the carboxylate functions to the longer wavelengths. The shift values are given in Table 6. The differences were of 12 and  $16 \text{ cm}^{-1}$  for the concentration of 0.5 and 1 g/l respectively. However, for 0.1 g/l, the shift was of  $3 \text{ cm}^{-1}$  equivalent of the shift of the spectrometer resolution. (iii) The vibration band elongation asymmetrical  $\nu_{\text{as}}$  ( $1590 \text{ cm}^{-1}$ ) of the carboxylate functions has been moved to the lowest wavelengths. There was a shift of 8, 20 and  $30 \text{ cm}^{-1}$  corresponding to the concentrations of 0.1, 0.5 and 1g/l, respectively. These shifts have confirmed previous results from other chemical analysis methods (Tables 4 and 6). The high concentration of 1 g/l caused a shift of  $30 \text{ cm}^{-1}$ , which means that there is an exchange easier between the elements  $\text{Na}^+$  and  $\text{Ca}^{2+}$  of the carboxylate function and  $\text{Hg}^{2+}$  and  $\text{Pb}^{2+}$  ions compared to the low concentrations of 0.1 and 0.5 g/l. In the case of mercury, the shift was of  $40 \text{ cm}^{-1}$  [15], we can see that this shift has dropped by  $10 \text{ cm}^{-1}$ , which proves that the cationic exchange becomes more difficult.

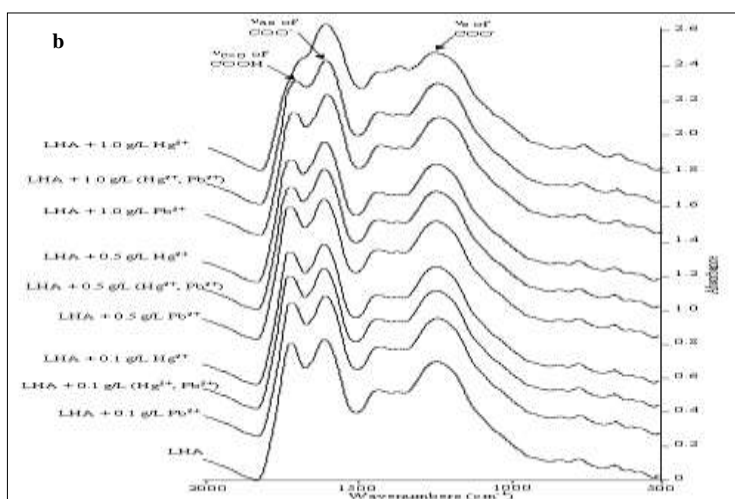
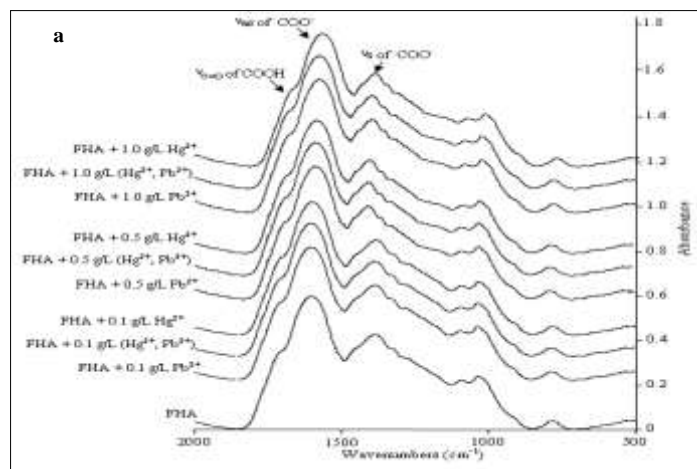


**Figure 5.** FTIR spectra of humic acids studied before and after interaction with mercury and lead:  
 (a) FHA and (b) LHA.

(iv) The  $\Delta v_{as-s}$  calculated values during the interaction of FHA with heavy metals are presented in Table 7. These values vary substantially with the nature of the metallic agent. It has observed that  $\Delta v_{as-s}$  follows the sequency:  $\Delta v_{as-s}(FHA-Hg) < \Delta v_{as-s}(FHA-(Hg,Pb)) < \Delta v_{as-s}(FHA-Pb)$ , indicating that the interaction between  $COO^-$  and  $Hg^{2+}$  is greater than that between  $COO^-$  and  $Pb^{2+}$ .

### III.4.2. Study of interactions LHA-binary (Hg-Pb)

#### III.4.2.1. Influence of the concentration of the mixed solution Hg-Pb

The adsorption rates in the LHA-Hg, LHA-Pb and LHA-Hg-Pb interactions are summarized in Table

6. We noticed that: (i) At low concentrations (0.1 g/l) of the binary solution, there is a significant adsorption of 95 and 91% for mercury and lead, respectively. (ii) At average concentrations (0.5 g/l), adsorption rates decreased by almost 3% compared to the study of the (LHA-single metal) interaction. (iii) At 1g/l of the mixed solution, the adsorption rates are of the order of 63% for mercury and 35% for lead. These values are lower compared to adsorption with FHA and LHA. The main reason for this phenomenon is the acid form of LHA.

**Table 7.** Frequencies, and maximum shift of the -COO<sup>-</sup> symmetric and asymmetric of the HA interaction with Hg [13], Pb [14] and Binary (Hg-Pb)

Humic Acid	Concentration Initial of métal	Adsorption system	ν <sub>as</sub> -COO <sup>-</sup> cm <sup>-1</sup>	ν <sub>s</sub> -COO <sup>-</sup> cm <sup>-1</sup>	Δν <sub>as-s</sub> -COO <sup>-</sup> cm <sup>-1</sup>	Maximum shift from the frequency of -COO <sup>-</sup> cm <sup>-1</sup>		Intensity of the C=O elongation vibration band of -COOH			
						ν <sub>as</sub>	ν <sub>s</sub>				
FHA	0 g/l	Blank	1590	1386	204	40	19	No variation			
	0.1 g/l	Hg	1580	1390	190			No variation			
		Pb	1584	1387	197			No variation			
		<b>Hg (Hg,Pb)</b>	<b>1582</b>	<b>1389</b>	<b>193</b>			<b>No variation</b>			
		<b>Pb (Hg,Pb)</b>	<b>1582</b>	<b>1389</b>	<b>193</b>			<b>No variation</b>			
	0.5 g/l	Hg	1565	1401	164			No variation			
		Pb	1575	1394	181			No variation			
		<b>Hg (Hg,Pb)</b>	<b>1570</b>	<b>1398</b>	<b>172</b>			<b>No variation</b>			
		<b>Pb (Hg,Pb)</b>	<b>1570</b>	<b>1398</b>	<b>172</b>			<b>No variation</b>			
	1.0 g/l	Hg	1550	1405	145			No variation			
		Pb	1566	1397	169			No variation			
		<b>Hg (Hg,Pb)</b>	<b>1560</b>	<b>1402</b>	<b>158</b>			<b>No variation</b>			
		<b>Pb (Hg,Pb)</b>	<b>1560</b>	<b>1402</b>	<b>158</b>			<b>No variation</b>			
	LHA	0 g/l	Blank	1610	1429			181	19	12	Appearance
		0.1 g/l	Hg	1608	1432			176			Decrease
			Pb	1607	1429			178			Decrease
<b>Hg (Hg,Pb)</b>			<b>1609</b>	<b>1431</b>	<b>178</b>	<b>Decrease</b>					
<b>Pb (Hg,Pb)</b>			<b>1609</b>	<b>1431</b>	<b>178</b>	<b>Decrease</b>					
0.5 g/l		Hg	1599	1436	163	Important decrease					
		Pb	1602	1431	171	Important decrease					
		<b>Hg (Hg,Pb)</b>	<b>1601</b>	<b>1433</b>	<b>168</b>	<b>Important decrease</b>					
		<b>Pb (Hg,Pb)</b>	<b>1601</b>	<b>1433</b>	<b>168</b>	<b>Important decrease</b>					
1.0 g/l		Hg	1591	1441	150	Almost total disappearance					
		Pb	1596	1394	202	Important decrease					
		<b>Hg (Hg,Pb)</b>	<b>1598</b>	<b>1439</b>	<b>159</b>	<b>Important decrease</b>					
		<b>Pb (Hg,Pb)</b>	<b>1598</b>	<b>1439</b>	<b>159</b>	<b>Important decrease</b>					

**III.4.2.2. Initial and final pH**

The values of the initial and final pH of interactions LHA -metal single LHA-binary are given in Table 6. Whatever the pH concentrations at the end of the LHA metal reaction alone or binary is always acid medium, of the order of 2-3.

**III.4.2.3. FTIR Spectroscopy monitoring**

The infrared spectra of the complex formed by LHA and the mixture Hg and Pb are shown in Figure 5b. The characteristics of the carboxylic function and the different attributions of bands related to the carboxylate function in LHA are

detailed in Table 4. Three principal bands were followed:

(i) The decrease in elongation vibration intensity ν<sub>C=O</sub> at 1709 cm<sup>-1</sup> of the carboxylic function reflects the increase in adsorbed metals. It can be deduced that the high concentration of the binary component solution (1g /l) did not cause the total disappearance of this band as in the case of the LHA interaction with the single component solution Hg (1 g/l).

(ii) The asymmetric elongation vibration band ν<sub>as</sub> at 1608 cm<sup>-1</sup> characteristic of the carboxylate function was shifted to the low wavenumber as a function of the increase in the number of metal cations. A small

displacement of about  $10\text{ cm}^{-1}$  was recorded for the 0.5 and 1 g/l concentrations of the binary solution Hg-Pb. This small displacement confirms that the active sites of LHA are not fully complexed.

(iii) The symmetrical elongation vibration band  $\nu_s$  characteristic of the carboxylate function was slightly shifted for both the 0.1 and 0.5 g/l concentrations. On the other hand, this shift was of the order of  $10\text{ cm}^{-1}$  for 1g/l.

(iv) The LHA interaction with the Hg solution has caused an important shift of  $\nu_{as}$  and  $\nu_s$  peaks of 19 and  $12\text{ cm}^{-1}$ , respectively (Table 7), therefore a shift rate of almost half compared to the FHA-Hg interaction ( $40$  and  $19\text{ cm}^{-1}$ ). This proves that the interaction between FHA-Hg is easier than the interaction between LHA-Hg. The shift values always follow the same order as in the case of the FHA-metal interaction:  $\Delta\nu_{as-s}(\text{LHA-Hg}) < \Delta\nu_{as-s}(\text{LHA-Hg-Pb}) < \Delta\nu_{as-s}(\text{LHA-Pb})$ .

### III.5. Selective affinity of adsorption of $\text{Hg}^{2+}$ and $\text{Pb}^{2+}$ cations

The results of this study are consistent with those found by other works [25,30,31]. The rate of fixation decreased in the case of the interaction of the organic matter (humic acid, lignite, etc.) with the mixed solutions (binary and tertiary) according to the work conditions:

- Liu et al. [25] have shown that adsorption capacities in the study of the peat-mono-component interaction ( $\text{Cu}^{2+}$ ,  $\text{Ni}^{2+}$  or  $\text{Cd}^{2+}$ ) fall with respect to competitive adsorption capacities in peat-multi-component ( $\text{Cu}^{2+}$ ,  $\text{Ni}^{2+}$ ), ( $\text{Cu}^{2+}$ ,  $\text{Cd}^{2+}$ ), ( $\text{Cd}^{2+}$ ,  $\text{Ni}^{2+}$ ) or ( $\text{Cu}^{2+}$ ,  $\text{Ni}^{2+}$ ,  $\text{Cd}^{2+}$ ).

- Zeledon-Toruno et al. [30] have observed a significant reduction in nickel uptake by LHA after the addition of a binary solution containing both metals ( $\text{Cu}^{2+}$ ,  $\text{Ni}^{2+}$ ).

- Peter et al. [31] concluded that silicate-immobilized humic material has greater selectivity for mercury. The order of affinity in a mixed solution (Hg, Pb, Cu) was classified as follows:  $\text{Hg}(\text{Hg}, \text{Pb}, \text{Cu}) > \text{Pb}(\text{Hg}, \text{Pb}, \text{Cu}) > \text{Cu}(\text{Hg}, \text{Pb}, \text{Cu})$ . In general, organic materials have a selective affinity for certain metals. This affinity has been linked to several factors such as: electronegativity [47], ionic potential ( $Z/r$ ) [48], reduction potential [41] and ionic radius [13]. Because of the small size of the  $\text{Hg}^{2+}$  ions (ionic radius,  $R_{\text{Hg}^{2+}} = 0.83\text{ \AA}$ ), mercury can create a great deal of competition in occupying the active sites of FHA and LHA compared to  $\text{Pb}^{2+}$  ions ( $R_{\text{Pb}^{2+}} = 1.33\text{ \AA}$ ). In addition, the degree of

association of the humic acids studied with Hg or Pb in the mixed solution is positively correlated with the reduction potential of  $\text{Hg}^{2+}$  ( $+0.8\text{ eV}$ ) which is greater than that of  $\text{Pb}^{2+}$  ( $-0.13\text{ eV}$ ). In at the same time, mercury has the highest affinity for FHA or LHA because it has an ionic potential greater than that of lead.

### IV. Conclusions

The study of the interaction between humic acid and metals using the FTIR spectroscopic technique has made possible the characterization of the main functions responsible for this interaction, such as the carboxylic and carboxylate functions. Indeed, it is sufficient to have at the start a humic acid whose FTIR spectra show the asymmetric  $\nu_{as}$  and the symmetric  $\nu_s$  elongations vibration band of  $-\text{COO}^-$  and  $\text{C}=\text{O}$  of the  $-\text{COOH}$  function. The displacement of  $\nu_{as}$  and  $\nu_s$  bands and the decrease of the peak intensity of the COOH function suggest a metal fixation. The frequency separations between the  $-\text{COO}^-$  asymmetric and symmetric stretches  $\Delta\nu_{as-s}$  strongly related to the type of the fixed metal. The results of this study showed the high adsorption capacity of humic acids for mercury compared to lead and the adsorption rate of FHA (salt form) is always higher than LHA (acid form). In this study we have added a fourth parameter  $\Delta\nu_{as-s}$  and found that:  $\Delta\nu_{as-s}(\text{HA-Hg}) < \Delta\nu_{as-s}(\text{HA-Hg-Pb}) < \Delta\nu_{as-s}(\text{HA-Pb})$ . The elimination rate of  $\text{Hg}^{2+}$  and  $\text{Pb}^{2+}$  in the binary case follows this sequence:  $\text{Hg}(\text{Hg-Pb}) > \text{Pb}(\text{Hg-Pb})$  due to the competition phenomenon between these two metallic ions, the mercury elimination rate by FHA and LHA has decreased by 10%.

As a result, the study makes it possible to quickly test with FTIR if the soil or humic acid is polluted with lead, mercury or both.

### Acknowledgements

The authors thank the Algerian National Administration of Scientific Research (DG-RSDT) for financial support.

### Conflicts of interest

There are no conflicts to declare.

## V. References

1. Bradl, H. Heavy Metals in the Environment: Origin, Interaction and Remediation; Academic Press: London; 10, 6(2002) 11.
2. Figueredo, F.G.; Lima, L.F.; Morais-Braga, M.F.B.; Figueredo, J.G.; Pinto, N.B.; Matias, E.F.F.; Menezes, I.R.A.; Almeida, R.S.; Cunha, F.A.B.; Coutinho, H.D.M. Potential assessment cytoprotective against toxic effect of chloride of mercury and antioxidant *Lygodium venustum* sw (lygodiaceae). *Revista Interfaces* 39 (2016a) 44-49.
3. Zhao, F.J.; Ma, Y.; Zhu, Y.G.; Tang, Z.; Mcgrath, S.P. Soil contamination in China: current status and 16 mitigation strategies. *Environmental Science and Technology* 49 (2015) 750-759. 17
4. Shixiang, W.; Yong, L.; Qin, F.; Anlan, Z.; Lu, F.; Yulan, M. Removal of Hg (II) from aqueous solution using sodium humate as heavy metal capturing agent. *Water Science and Technology* 74 (2016) 2946-2957.
5. Zhang, Y.; Du, J.; Ding, X.; Zhang, F. Comparison study of sedimentary humic substances isolated from contrasting coastal marine environments by chemical and spectroscopic analysis. *Environmental Earth Sciences* 75 (2016) 378.
6. Gondar, D.; López, R.; Fiol, S.; Antelo, J.; Arce, F. Cadmium, lead, and copper binding to humic acid and 23 fulvic acid extracted from an ombrotrophic peat bog. *Geoderma* 135 (2006) 196-203.
7. Liu, A.; Gonzalez, R.D. Modeling Adsorption of Copper (II), Cadmium (II) and Lead(II) on Purified Humic Acid. *Langmuir* 16 (2000) 3902-3909. 26
8. Covelo, E.F.; Andrade, M.L.; Vega, F.A. Heavy metal adsorption by humic umbrilsols: selectivity sequences and competitive sorption kinetics. *Journal of Colloid and Interface Science* 280 (2004) 1-8.
9. Plaza, C.; Brunetti, G.; Senesi, N.; Polo, A. Molecular and Quantitative Analysis of Metal Ion Binding to Humic Acids from Sewage Sludge and Sludge-Amended Soils by Fluorescence Spectroscopy. *Environmental Science and Technology* 40 (2006) 917-923.
10. Janos, P.; Sypecka, J.; Mlckovska, P.; Kuran, P.; Pilarova, V. Removal of metal ions from aqueous solutions by sorption on to untreated low-rank coal (oxihumolite). *Separation and Purification Technology* 53 (2007) 322-329.
11. Kulikowska, D.; Gusiatin, Z.M.; Bulkowska, K.; Klik, B. Feasibility of using humic substances from compost to remove heavy metals (Cd, Cu, Ni, Pb, Zn) from contaminated soil aged for different periods of time. *Journal of Hazardous Materials* 300(2015) 882-891.
12. Rong, Q.; Zhong, K.; Huang, H.; Li, C.; Zhang, C.; Nong, X. Humic Acid Reduces the Available Cadmium, Copper, Lead and Zinc in Soil and Their Uptake by Tobacco. *Applied Sciences* 10 (2020) 1077.
13. Terkhi, M.C.; Taleb, F.; Gossart, P.; Semmoud, A.; Addou, A. Fourier transform infrared study of mercury interaction with carboxyl groups in humic acids. *Journal of Photochemistry and Photobiology A* 198 (2008) 205-214.
14. Gossart, P.; Semmoud, A.; Ouddane, B.; Huvenne, J.P. Study of the interaction between humic acids and lead: exchange between  $Pb^{2+}$  and  $H^+$  under various chemical conditions followed by FTIR. *Physica and Chemical News* 9 (2003) 101-108.
15. Santoso, U.T.; Santosa, S.J.; Siswanta, D.; Rusdiarso, B.; Shimazu, S. Characterization of sorbent produced through immobilization of humic acid on Chitosan using glutaraldehyde as cross-linking agent and Pb(II) ion as active site protector. *Indonesian Journal of Chemistry* 10 (2010) 301-309.
16. Shulten, H.R.; Shnitzer, M. A state of the art structural concept for humic substances. *Natur Wissen schaften*. 80 (1993) 29-30.
17. Sparks, D.L. Environmental soil chemistry, Academic Press, New York, 1995.
18. Hayes, M.H.B. Humic substances in soil, sediment and water. Wiley, New York, 1985.
19. Schnitzer, M.; Gupta, U.C. Determination of acidity in soil organic matter. *Soil Science Society of America Journal* 29 (1965) 274-277.
20. Cherifi-Naci, H.; Boughrara, S.; Louhab, K. Efficacité des argiles à piliers d'oxydes d'aluminium et de fer pour l'élimination du Cu (II) à partir des solutions aqueuses. *Algerian Journal of Environmental Science and Technology* 3 (2015) 74-82.
21. Djebri, N.; Boukhalfa, N.; Boutahala, M.; Chelali, N. Préparation des biomatériaux d'hydrogels à base d'argile et d'alginate (algues brunes): application environnementale. *Algerian Journal of Environmental Science and Technology* 3 (2017) 532-538.
22. Behilila, A.; Lahcenea, D.; Zahraouia, B.; Benmehdia, H.; Belhachemia, M.; Choukchou-Braham, A. Dégradation d'un colorant cationique par la photocatalyse solaire à travers une argile algérienne imprégnée avec TiO<sub>2</sub>. *Algerian Journal of Environmental Science and Technologie* 3 (2020) 1566-1574.
23. Nara, M.; Torii, H.; Tasumi, M. Correlation between the vibrational frequencies of the carboxylate group and the types of its coordination to a metal ion: An ab Initio. Molecular Orbital Study. *Journal of Physical Chemistry* 100 (1996) 19812-19817.
24. Toubal, S.; Elhaddad, Dj.; Bouchenak, O.; Yahiaoui, K.; Sadaoui, N.; Arab, K. L'importance des extraits d'*Urtica dioica* L. dans la lutte contre *Culex pipiens* (Linné, 1758). *Algerian Journal of Environmental Science and Technology* 5 (2019) 868-872.
25. Liu, Z.; Zhou, L.; Wei, P.; Zeng, K.; Wen, C.; Lan, H. Competitive adsorption of heavy metal ions on peat. *Journal of China University of Mining and Technology* 18 (2008) 255-260.
26. Bosire, G.O.; Kgarebe, B.V.; Ngila, J.C. Experimental and theoretical characterization of metal complexation with humic acid. *Analytical Letters* 49 (2016) 2365-2376.
27. Steelink, C. Implications of elemental characteristics of humic substances. In G. Aiken, D. McKnight, R. Wershaw and P. MacCarthy, (eds.), *Humic Substances in Soil, Sediment and Water*. Wiley Interscience, New York, 1985.
28. Qian, L.B.; Chen, B.L. Dual role of biochars as adsorbents for aluminium: the effect of oxygen containing organic components and the scattering of silicate particles. *Environmental Science and Technology* 47 (2013) 8759-8768.
29. Babel, S.; Kurniawan, T.A. Low-cost adsorbents for heavy metals uptake from contaminated water: a review. *Journal of Hazardous Materials* 97 (2003) 219-243.
30. Zeledon-Toruno, Z.; Lao-Luque, C.; Solé-Sardans, M. Nickel and copper removal from aqueous solution by an immature coal (leonardite): effect of pH, contact time and water hardness. *Journal of Chemical Technology and Biotechnology* 80 (2005) 649-656.
31. Peter, C.S.; Gary, D.R. Competitive metal binding to a silicate-immobilized humic material. *Journal of Hazardous Materials* 145 (2007) 203-209.
32. McKay, G.; Porter, J.F. Equilibrium parameters for the sorption of copper, cadmium, and zinc ions onto peat. *Journal of Chemical Technology and Biotechnology* 69 (1997) 309-320.

33. Allen, S.J.; Brown, P.A. Isotherm analyses for single component and multi-component metal sorption onto lignite. *Journal of Chemical Technology and Biotechnology* 62 (1995) 17-24.

**Please cite this Article as:**

Terkhi M.C., Ghezzar M.R., Addou A., Rapid detection by FTIR spectroscopy of the competition of Hg (II) and Pb (II) on the functional sites of humic acid, *Algerian J. Env. Sc. Technology*, **8:4 (2022) 2703-2719**